BNL 30185

CONF-8107S9--5

LOW-p_t PHYSICS

P.L. Braccini - CERN
L-L. Chau - BNL
G. Giacomelli - U. of Bologna
M. Valdata-Nappi - U. of Pisa
T.F. Kycia - BNL
S.J. Lindenbaum - BNL
R.S. Longacre - BNL

I. INTRODUCTION

This group examined the processes with large cross sections, namely total cross sections, elastic scattering, particle production at low p_t and diffraction excitation. These are fundamental processes whose experimental study has always been one of the main aims of the physics program of each new accelerator in a new energy domain.

The main features of these large cross section processes may be studied experimentally using relatively simple set ups at an early stage of phase I Isabelle operation.[1] Luminosities of $\simeq 10^{30}$ cm^{-2}sec^{-1} are quite adequate to perform precision experiments. Higher luminosities will be needed to study elastic scattering at larger angles, particle production at medium values of p_t and the production of new flavour.

The large cross section processes are characterized by features which change slowly, logarithmically with c.m. energy (ln s physics). The new large range of energies which will become available at Isabelle will allow the possibility of performing a detailed study of the energy dependences of the processes under consideration. It will also be possible to perform detailed comparisons with similar experiments in $\bar{p}p$ collisions.

II. TOTAL CROSS SECTION AND ELASTIC SCATTERING AT SMALL ANGLES

The measurement of the elastic differential cross section at small momentum transfer t may be used to determine the imaginary part of the forward

non-spin-flip part of the nuclear scattering amplitude, which, through the optical theorem, gives the total cross section. The forward real part may be determined from the study of elastic scattering in the Coulomb-nuclear interference region or from total cross sections via dispersion relations.

The total cross section, (σ_{tot}), and the ratio of the real to imaginary part of the forward scattering amplitudes (ρ) characterize our knowledge of this field. Figure 1 shows a compilation of pp and $\bar{p}p$ total cross sections and of ρ-values for pp interactions.[2] The energy dependence of the pp total cross section is known: after having reached a broad minimum, around $\sqrt{s}$ = 12 GeV, it rises with a dependence which is not well established, but could be of the $\ln^2 s$ type. $\bar{p}p$ cross sections have reached a plateau at $\sqrt{s}$ > 20 GeV. As the energy increases ρ_{pp} goes from negative to positive values. The full curves in Fig. 1 represent results of fits to the experimental points; the shaded areas represent extrapolations located within one standard deviation.

New measurements of σ_{tot} and ρ in $\bar{p}p$ collisions will presumably become available from the CERN ISR and SPS colliders (up to $\sqrt{s}$ = 540 GeV) and later from the Fermilab collider (up to 1600-2000 GeV).

One would like answers to the following questions: Will $\sigma_{tot}(pp)$ keep increasing? If so with which s-dependence? Is ρ_{pp} going to reach a maximum and start decreasing towards zero? Are there new thresholds in the total cross section? When will $\sigma_{tot}(pp)$ become equal to $\sigma_{tot}(\bar{p}p)$? Can we understand theoretically the rise in σ_{tot}? In fact our understanding of this field is limited and proceeds via specific models.[2,3] Figure 2 shows examples of predicted energy dependences for $\sigma_{tot}(pp)$ and $\sigma_{tot}(\bar{p}p)$ at higher energies.

It is clear that to answer these questions one needs precision measurements at higher energies. Here Isabelle plays an important role.

ρ and σ_{tot} are best obtained from a combination of measurements:[4]

i) elastic scattering in the C-N interference region ($10^{-3} < |t| < 10^{-2}$ $(GeV/c)^2$) (the cross section depends on ρ, σ_{tot} and on the slope of the diffraction pattern b);

ii) measurement of σ_{tot} from the total interaction rate;

iii) simultaneous measurements of total interaction rate and elastic scattering in the Coulomb-Nuclear interference region;

iv) from elastic scattering at slightly larger angles.

A single interaction region could be used for simultaneous measurements of (i) the elastic scattering in the $10^{-3} < |t| < 10^{-1}$ $(GeV/c)^2$ region, (ii) the total collision rate (iii) elastic scattering at intermediate t.

Figure 3 represents a simple conceptual sketch of how the experiments might be arranged. It is clear that they might be done very differently.

It has been emphasized that for these measurements it is important to have stable clean beams, with very low angular divergence ($\lesssim 0.03$ mrad in the crossing region). A luminosity of 10^{29} $cm^{-2}sec^{-1}$ could be adequate, but it has to be known with good accuracy. As demonstrated at the CERN-ISR a simultaneous measurement of the total interaction rate, of the forward elastic rate and of the luminosity via the Van de Meer method are necessary to obtain results at the level of 1% accuracy.

The measurements should be done at a number of different primary energies.

III. ELASTIC SCATTERING

The main features of the differential cross section for pp elastic scattering for $|t| > 0.01$ $(GeV/c)^2$ and for $20 < \sqrt{s} < 63$ GeV are: (i) a narrow peak at small angles, probably with two slopes; (ii) a dip at $|t| \approx 1.4$ $(GeV/c)^2$, followed by a peak at $|t| \approx 2$; (iii) a small cross section, still

decreasing rapidly, at larger angles. As the energy increases the slope (or slopes) of the forward peak becomes steeper (shrinking of the forward peak), while the location of the dip moves towards smaller t-values (Fig. 4).

Data for $\bar{p}p \to \bar{p}p$ concern only low energies (see Fig. 5).

For experimental reasons we may divide the angular pattern in three regions, for $|t| < 0.05$ (CN interference region; it has already been discussed in Section 2), $0.05 < |t| < 1$ (diffraction region proper) and $|t| > 1$ (large angle region).

The data on elastic scattering are mostly interpreted in terms of optical models, geometric scaling, etc., all of which emphasize some aspects.[3] In the geometrical description of diffractive scattering the number and locations of the dips are related to the value of the total cross section.[3] Only the first dip was seen in both pp and $\bar{p}p$ interactions. The location in t of the first dip should decrease as σ_{tot} increases, in agreement with current pp and $\bar{p}p$ data. At the energies of the CERN and Fermilab $\bar{p}p$ colliders and of Isabelle, the total cross sections for $\bar{p}p$ and pp are expected to be about the same and to increase with energy. Therefore, the motion of the first dip for both pp and $\bar{p}p$ should be the same. The second dip, if seen, should have a similar motion.

Both the first and second dip should be observed at the three mentioned accelerators. It is instead unlikely that the third dip will be seen.

With experiments on elastic scattering at Isabelle one would like to answer the following questions:

i) What is the exact t-dependence of elastic scattering in the diffraction region proper?; is the slope b a function of t?

ii) Will shrinking continue? how fast? Will one eventually have equal slopes for pp and $\bar{p}p$ elastic scattering, $b(pp) = b(\bar{p}p)$?

iii) Is the dip-bump structure at 1.5-2 $(GeV/c)^2$ of defractive type? If so, why does one not see a second minimum? What happens at $|t| > 10$ $(GeV/c)^2$?

iv) Does $\bar{p}p$ have a behavior similar to pp?

Experiments at Isabelle using relatively simple equipment, should provide many answers to the above questions.

We have already discussed the elastic scattering at $|t| < 0.05$ $(GeV/c)^2$. The study of scattering in $0.05 < |t| < 1$ GeV could be performed easily measuring only the angles of the scattered protons for scattering in the vertical plane; at larger angles the elastic cross section becomes considerably smaller so that also momenta have to be measured in order to separate elastic scattering from the inelastic. Two correlated spectrometers (as sketched in Fig. 3) can easily measure elastic scattering. The spectrometers can be short if the chambers have good spatial resolutions ($\sim$ 0.2 mm). For measurements for $|t| < 1$ there is no rate problem. The dip-bump structure in the elastic scattering can be measured with luminosities of a few times 10^{30}; for $t > 5$ GeV one needs instead $L > 10^{31}$ $cm^{-2}sec^{-1}$.

IV. PARTICLE PRODUCTION-SINGLE INCLUSIVE SPECTRA

It may be worthwhile recalling that at $\sqrt{s} = 53$ GeV the total cross section is $\sim$ 40 mb, the elastic cross section is $\sim$ 7 mb, the diffractive processes cross section is $\sim$ 10 mb and the inelastic non-diffractive is $\sim$ 23 mb. Extensive measurements on single inclusive spectra have shown:

i) A slow increase with energy of multiplicities of the produced particles, which consist mainly of pions (Fig. 6). At $\sqrt{s} = 700$ GeV one expects $\langle n_{ch} \rangle \sim$ 25-30, 90% of which should be pions.

ii) Limited transverse momentum of the secondaries; typically one has an exponential decrease with $\langle p_t \rangle \sim 0.35$ GeV/c (See Fig. 7).

iii) Approximate scaling of the inclusive cross sections. From the plot of Fig. 8 in terms of laboratory rapidity one expects an increase of the invariant cross section at y = 0 of about 40%.

These features are explained in most theoretical models of particle productions, though there is, to our knowledge, no model which satisfactorily explains all of them.

In conjunction with the above points one will like to know:

i) What is the energy dependence of the charge multiplicity? Will it become of a simple lns type?

ii) For low p_t what is the shape of the invariant cross section (exponential, gaussian, ...)? Does the average value of p_t reach a constant value or increase with s?

iii) When a large rapidity range is available, as will be at Isabelle, does one have a real rapidity plateau in cross section, or does the y = 0 cross section keep increasing?

The general features of inclusive production of long lived charged hadrons may be easily obtained using single arm spectrometers. One needs at least two such spectrometers, one at very small angles and one at large angles, around 90°. In order to achieve good particle identification, spectrometers have to be instrumented with Cerenkov counters, time of flight counters, and new types of detectors, like transition radiators and dE/dx chambers.

The small angle spectrometer may be placed in the same narrow angle hall together with the total cross section and elastic scattering set ups.[5] The spectrometer should be able to handle ≈ 360 GeV/c particles, which means

that the spectrometer may be very long because of the need of long Cerenkov counters and long lever arms. The use of transition radiation detectors and dE/dx chambers in place of Cerenkov counters and the use of high resolution tracking chambers would allow a considerable reduction in the length of the spectrometer.

One could also consider a medium-angle single-arm spectrometer used in conjunction with the intermediate-t elastic scattering set up.

In order to complete the survey of inclusive production one may also consider: (a) the use of a set of lead glass counters to measure the inclusive yield of γ's (and therefore of π^0 mesons), (b) a neutron calorimeter to measure (at small angles) the inclusive yield of neutrons. Both are sketched in Fig. 3.

V. CORRELATIONS AT LOW p_t

A dominant feature of particle production at low p_t is the presence of short range correlations in rapidity, with a correlation length of about 2 units of rapidity (see Fig. 9). These and other types of correlations were extensively studied at the ISR, and were interpreted in the framework of various theoretical models - in particular the cluster model. The average features of each cluster (mean charged multiplicity $\simeq$ 1.8, average mass $\simeq$ 1.3 GeV, average transverse momentum $\simeq$ 0.65 GeV) are not too dissimilar from those of a resonance; it may be that most of the clusters are resonances. It is in fact known (mainly from high energy bubble chamber experiments) that most pions are not produced directly, but come from the decay of resonances. If we limit the discussion to the simplest rapidity correlations, one may ask the following questions: at higher energies does one still have short range rapidity correlations with the same correlation length? And what

about rapidity correlations among identified particles, i.e., Kπ, Kp, etc.? Also: do long-range rapidity correlations exist?

In order to perform pseudo-rapidity correlations among charged particles one needs a large solid angle apparatus, which detects charged particles with a reasonable θ resolution. The scintillation counters and/or the wire chambers surrounding the interaction region as shown in Fig. 3 for the measurement of the total cross sections may be satisfactory. If, instead, one wants also the sign of the particles one needs a magnetic field over a large region and the set up becomes complex, as is described in the next section. Rapidity correlations of charged particles with π^0's and neutrons could instead be done still with the set ups indicated in Fig. 3.

VI. CHARACTERISTICS OF MULTIPARTICLE PRODUCTION

The bulk of the measureable inelastic cross section at Isabelle energies will be composed of multiparticle events with low p_t. In the context of QCD these events would be produced by soft QCD processes. A systematic study of their characteristics could be accomplished using a large solid angle multiparticle spectrometer with charged particle identification capability and γ-ray detection capability.

A description of a proposed spectrometer system for Isabelle, sketched in Fig. 10, is appended.[6] It has novel features, like fast charged particle identification based on ionization loss and transition radiation detector chambers.[7,8] In addition relatively cheap particle tracking detector systems with magnetic momentum determination are possible using new narrow gap drift chamber systems technology, which was recently developed at BNL for MPS II.[8]

The spectrometer may identify p, $\bar{p}$, $K^{\pm}$, $\pi^{\pm}$, and the γ-rays from π^0 decays in the low to medium p_t region. It will also have good momentum

resolution and will be sensitive to the identification of particles with $Q \neq 1$, for example quarks, etc.

With a spectrometer of this type one may study many processes, some of which are listed below.

1. Multiparticle event and jet behavior as a function of p_t and of x of each particle. Since one will be identifying individual particles the detailed differences in the behavior of different particle types can be studied as a function $f(p_t,x,s)$. For example, it may be possible to observe differences in quark and gluon jets as their production is varied from soft QCD to hard QCD processes.

2. Particle correlations, clusters and the hadronization process. One can study jet production with trigger selection of cluster formations, and observe in detail the content of the cluster in terms of known and possibly new resonances. Since many particles will be detected, one can do two and even more than two particle correlation studies.

Another possibility is a search for glueballs.[10] It has been pointed out that Isabelle may be a "glueball factory", since gluons dominate the evolution of QCD jets and low mass color singlet gluon pairs may be found at the end of a gluon cascade.

3. At Isabelle energies diffractive dissociation is expected to have a several mb cross section. One would expect to excite heavy N^* systems, some of which should decay into particles which contain heavy quarks - old and possibly new. Lepton triggers in the forward direction should preferentially select this type of event.

Cosmic ray experiments have found so-called "Centauro events" at modest p_t, which are characterized by a marked absence of π^0's compared

to charged particles. This spectrometer system may detect such events if they exist at Isabelle.

4. Search for Quarks. The dE/dx identifiers will be particularly sensitive for selecting quarks. One can reach high p_t as well as low p_t by rearranging the spectrometer as necessary. Any $Q \neq 1$ particle could be identified by this system provided Q is not too close to 1.

5. One particle inclusive physics with particle identification. Multiparticle inclusive physics, for instance resonance production, can also be done.

6. p-p elastic scattering from low t out to moderate and even high t can be done with a system of this sort, possibly involving some addition or rearrangements.

7. One can study the polarization of Λ^0 as a function of p_t and s. This can serve as a test of QCD.

REFERENCES

1. See previous Isabelle Workshops, for instance: C. Chang, et al., (Review of Experiments) 1977 Isabelle Workshop, p. 309; J.N. Marx, et al., (Measuring Coulomb-Nuclear Interference as a first round ISA Experiment), p. 204 (1975); P. Limon, et al., (Elastic Scattering and Diffraction Dissociation in the Angular range 0-50 mrad), p. 188 (1976); C. Y. Chang, et al., (Small Angle Arm Spectrometer for Isabelle), p. 244 (1975); H. Jöstelin, et al., (A Proposal for Combining a Large Detector Facility with the Small Angle Area), p. 209 (1978); S.U. Chung, et al., (A 4π Experiment for Isabelle, p. 183 (1975).
2. G. Giacomelli and M. Jacob, Phys. Repts. 55, 1 (1979). G. Giacomelli (High Energy Hadronic Interactions) Lectures at the 1980 Scottish Summer School.
3. See for example, T.T. Chou and Chen Ning Yang (Dip Movement in $\bar{p}p$ and pp collision), Phys. Rev. Lett. 46, 764 (1981); R. Horgan, et al., (Physics at Collider Energy) CERN-DESY School of Physics (1980).
4. M. Battiston, et al., (The Measurement of Elastic Scattering and of the Total Cross Section at the CERP $\bar{p}p$ collider) CERN-SPSC/78-105 (1978).
5. S. Aronson, et al., (Design Criteria for the 2 O'clock Experimental rea at Isabelle) Technical Note No. 125 (1979).

6. S.J. Lindenbaum and R.S. Longacre, A Multiparticle Magnetic Spectrometer with dE/dx and TRD Particle Identification, these proceedings.
7. T. Ludlam, et al., IEEE Trans. on Nucl. Sci. NS-28, 439 (1981).
8. T. Ludlam, et al., "Particle Identification by Electron Cluster Detection of Transition Radiation Photons", Nucl. Instr. and Meth. (in press); C.W. Fabjan, et al., "Practical Prototype of a Cluster Counting Transition Radiation Detector", submitted to Nucl. Instr. and Meth.
9. E.D. Platner, IEEE Trans. on Nucl. Sci. NS-25, 35 (1978); A. Etkin and M.A. Kramer, IEEE Trans. on Nucl. Sci. NS-27, 139 (1980).
10. J.F. Donoghue and F. Fishbane, Orbis Scientiae, to be published; J.F. Donoghue, Proc. of the 1980 Madison Conf.; S.J. Lindenbaum, The OZI Rule and Glueballs, Nuovo Cimento, to be published. S.J. Lindenbaum, QCD, OZI and Evidence for Glueballs, XVI Recontre De Moriand Particle Physics Meeting, March 15-27, 1981, to be published in the proceedings.

FIGURE CAPTIONS

Fig. 1. (a) compilation of ρ-values for pp scattering and (b) total cross sections for pp and $\bar{p}p$. The full curves are the results of a fit performed simultaneously on σ_{tot} and ρ. The shaded areas represent the one standard deviation region for ρ and the cross sections. The boundaries of these regions were obtained by changing the high energy behaviour of the cross sections in such a way that the χ^2 of the fit increased by one.

Fig. 2. Comparison of three parametrizations fitted to total cross section data above 8 GeV/c.

Fig. 3. Conceptual sketch of a possible layout of various set ups in the narrow intersection region at 2 o'clock. 1) Detectors for elastic scattering in the C-N interference region (Roman pots); 2) Total rate and luminosity detectors; 3) Elastic scattering detectors; 4) Small angle spectrometer; 5) Large angle spectrometer; 6) lead glass detectors; 7) neutron calorimeter.

Fig. 4. Differential cross-section for pp elastic scattering at ISR energies.[2]

Fig. 5. Differential cross-section for $p\bar{p}$ elastic scattering at 50 GeV incident energy.[4]

Fig. 6. The average multiplicity obtained by integrating inclusive distributions of π^+, π^-, K^+, K^-, p, $\bar{p}$ and for all charged particles, plotted as a function of s. Dashed lines represent the results of the fits to the formula $\langle n_i \rangle = A + B \ln s + Cs^{-\frac{1}{2}}$ (R202).

Fig. 7. Average transverse momentum for the production of pions, kaons, antiprotons and all charged particles plotted versus lab momentum. On the right are shown "temperature" scales for different particles, computed in the framework of the thermodynamic model (R202).

Fig. 8. Inclusive rapidity distributions for different particles at $p_t = 0.4$ GeV/c. Data points cover the full ISR energy range.

Fig. 9. Rapidity correlations for two charged particles at the two extreme ISR energies. The ridge along the main diagonal stands for short-range correlations associated with the production of uncorrelated clusters. Results from the Pisa-Stony Brook Collaboration at the ISR.

Fig. 10. Conceptual sketch of a multiparticle magnetic spectrometer with ionization loss and transition radiation particle identification.[5] Correcting

magnets must be used on the opposite side of the intersection. A second spectrometer will be located on that other side.

The dotted spectrometer at right angles to the beam is an example of how this type of spectrometer could be used for wide angle physics. An opposite arm could also be used. Another example would be placing a magnet right over the intersection region and instrumenting both sides.

ISABELLE

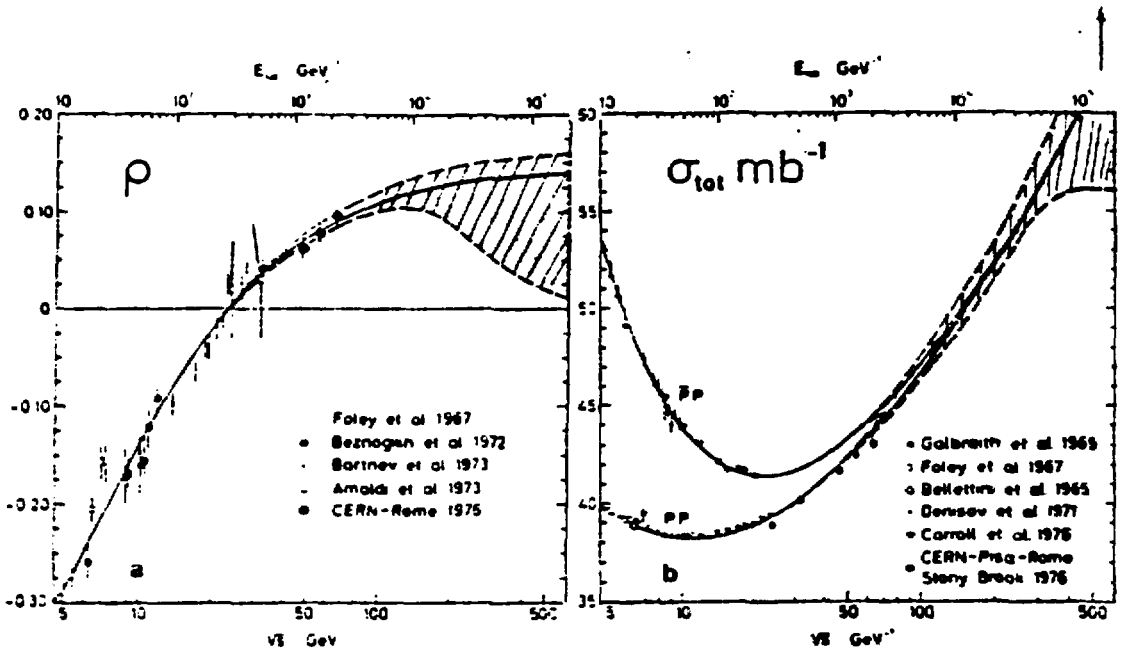

Fig. 1

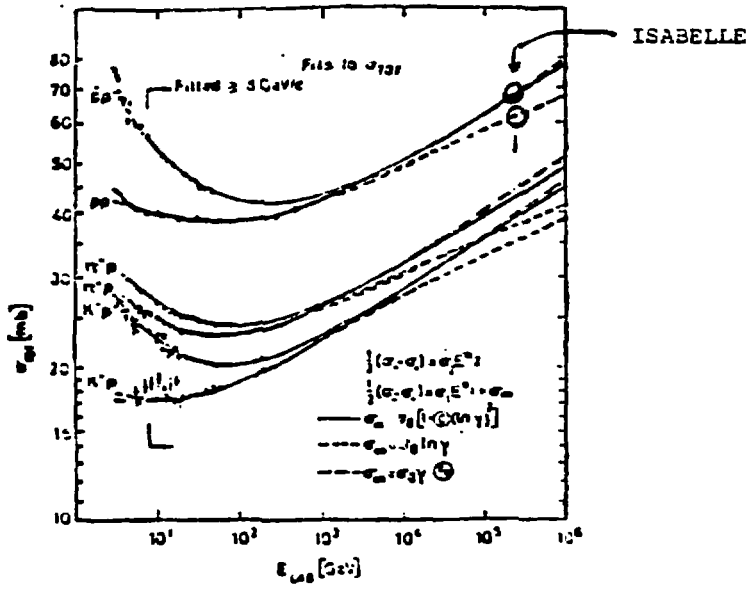

Fig. 2

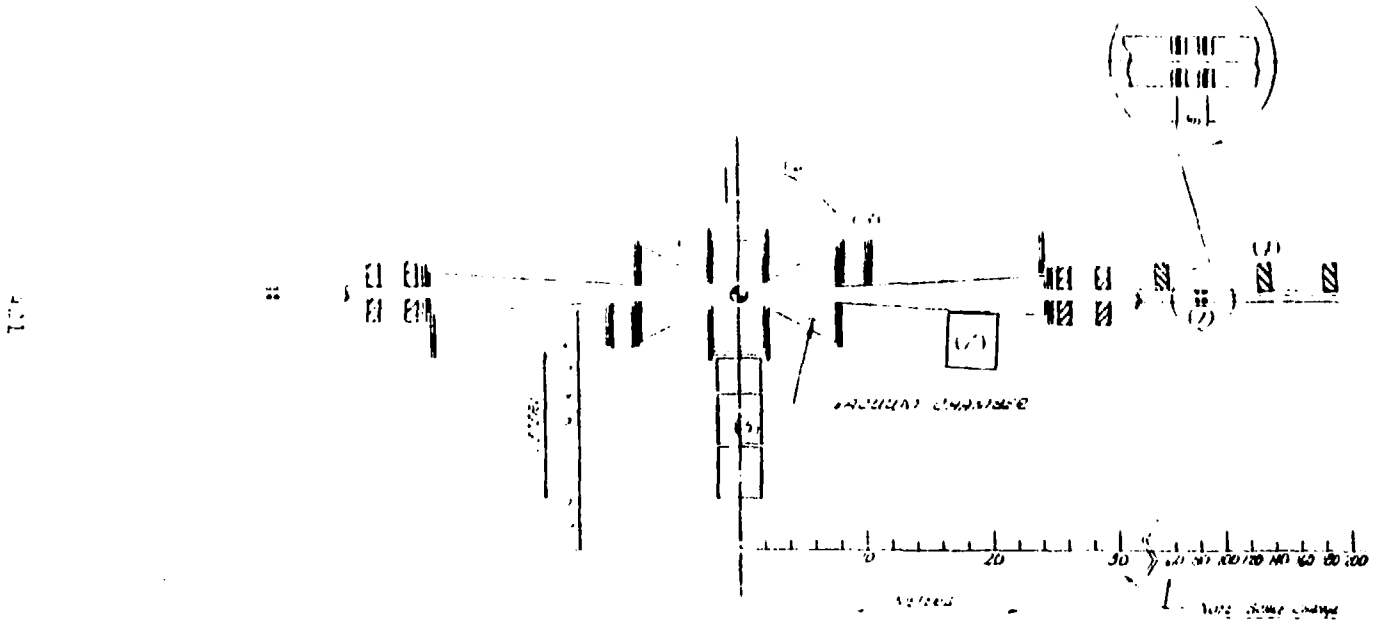

Fig. 3

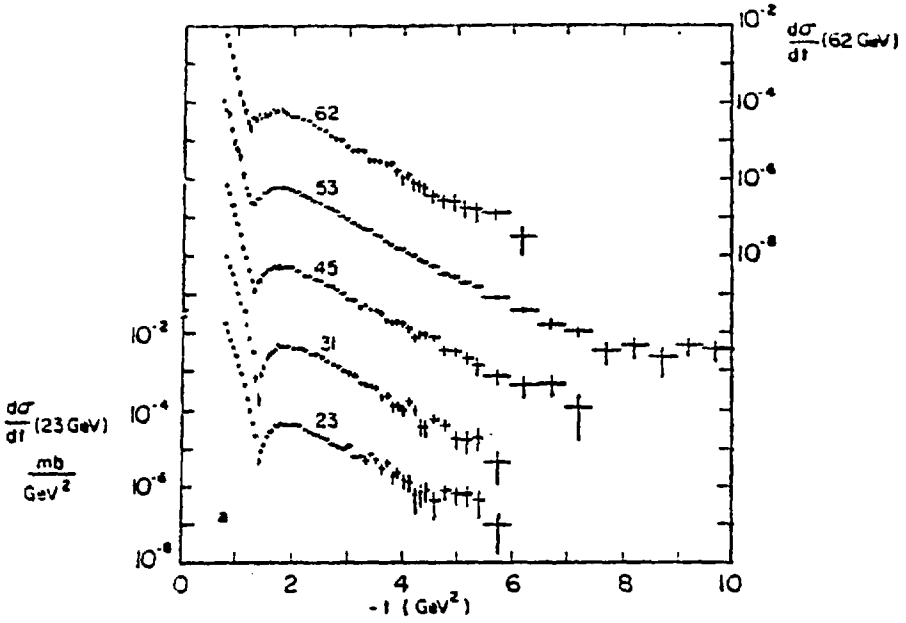
62
53
45
31
23
a
$\frac{d\sigma}{dt}$(23 GeV)
$\frac{mb}{GeV^2}$
$\frac{d\sigma}{dt}$(62 GeV)
10^{-2}
10^{-4}
10^{-6}
10^{-8}
0
2
4
6
8
10
$-t\ (GeV^2)$

Fig. 4

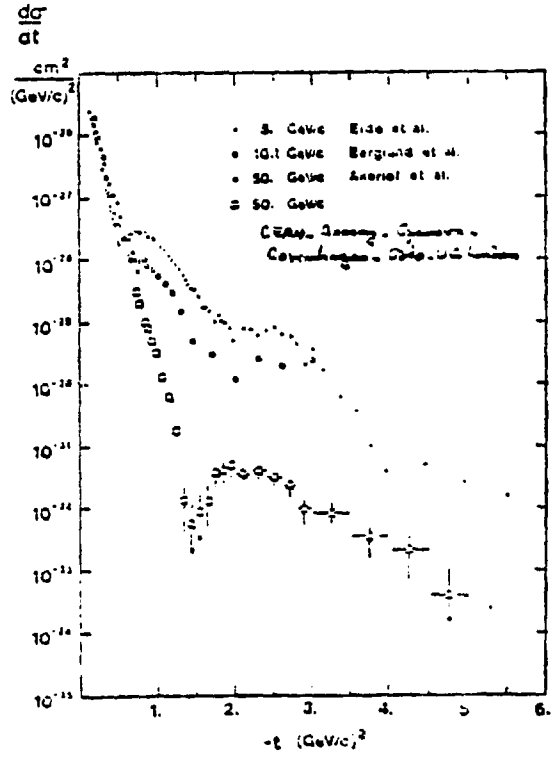
$\frac{d\sigma}{dt}$
$\frac{cm^2}{(GeV/c)^2}$
10^{-26}
10^{-27}
10^{-28}
10^{-29}
10^{-30}
10^{-31}
10^{-32}
10^{-33}
10^{-34}
10^{-35}
1.
2.
3.
4.
5
6.
$-t\ (GeV/c)^2$

Fig. 5

ISABELLE

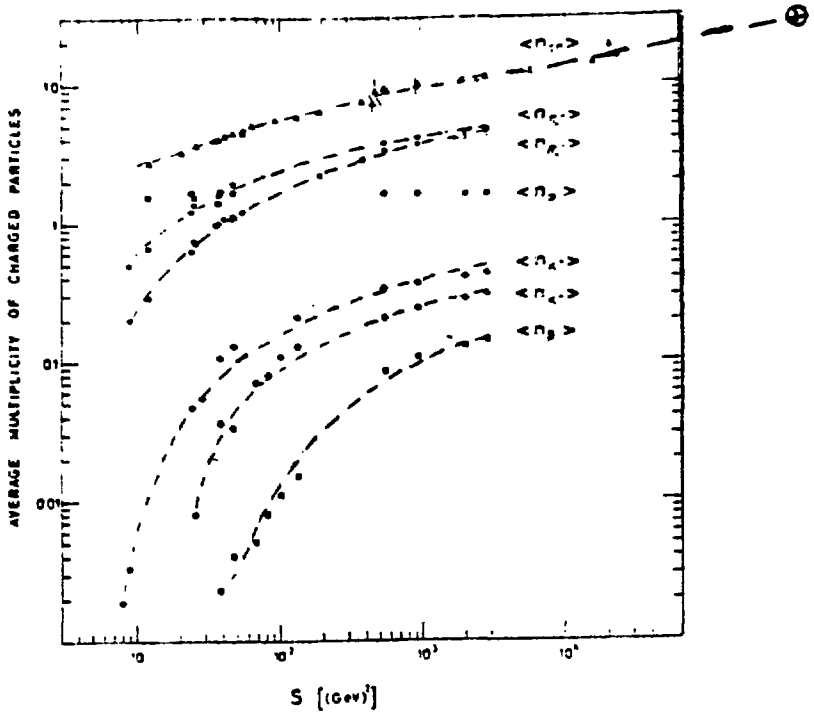

Fig. 6

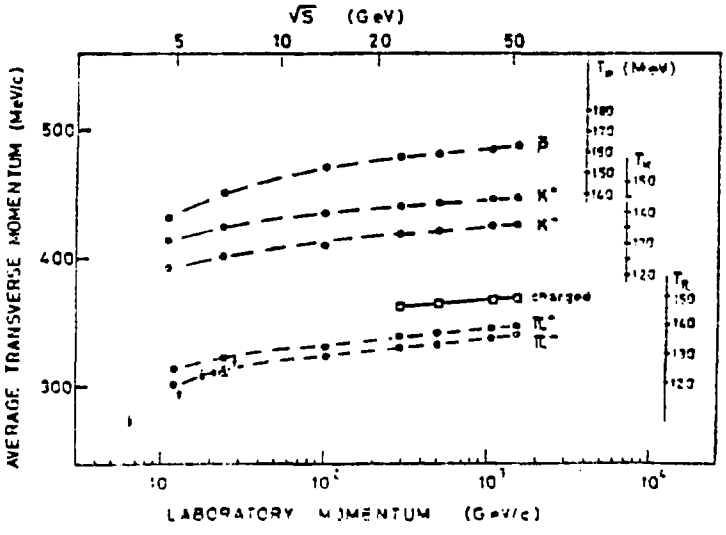

ISABELLE

Fig. 7

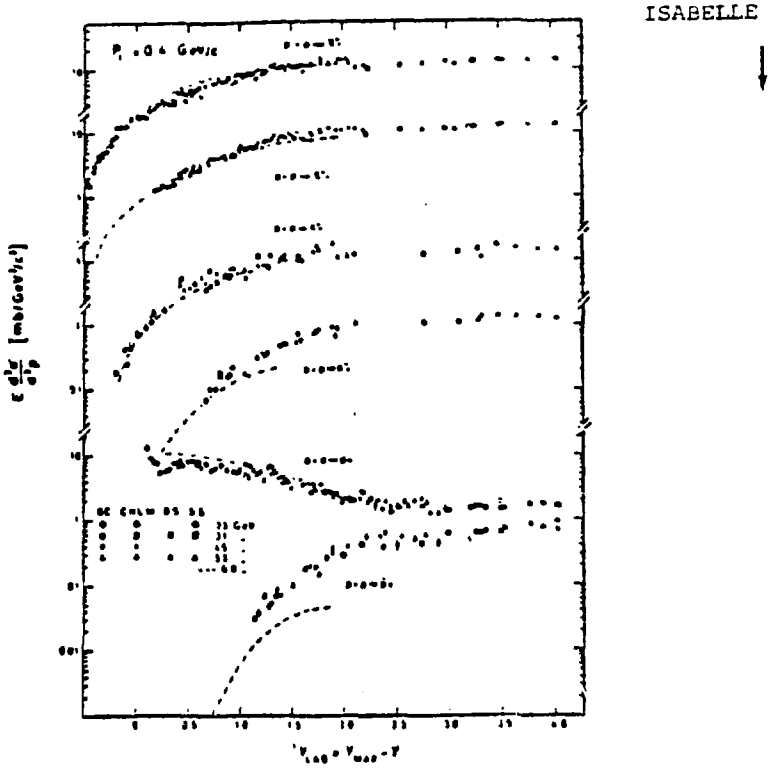

Fig. 8

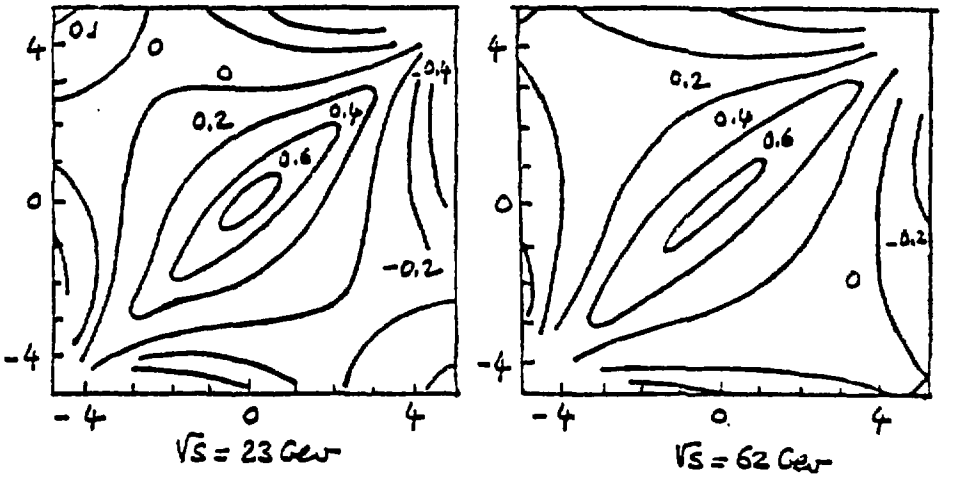

Fig. 9

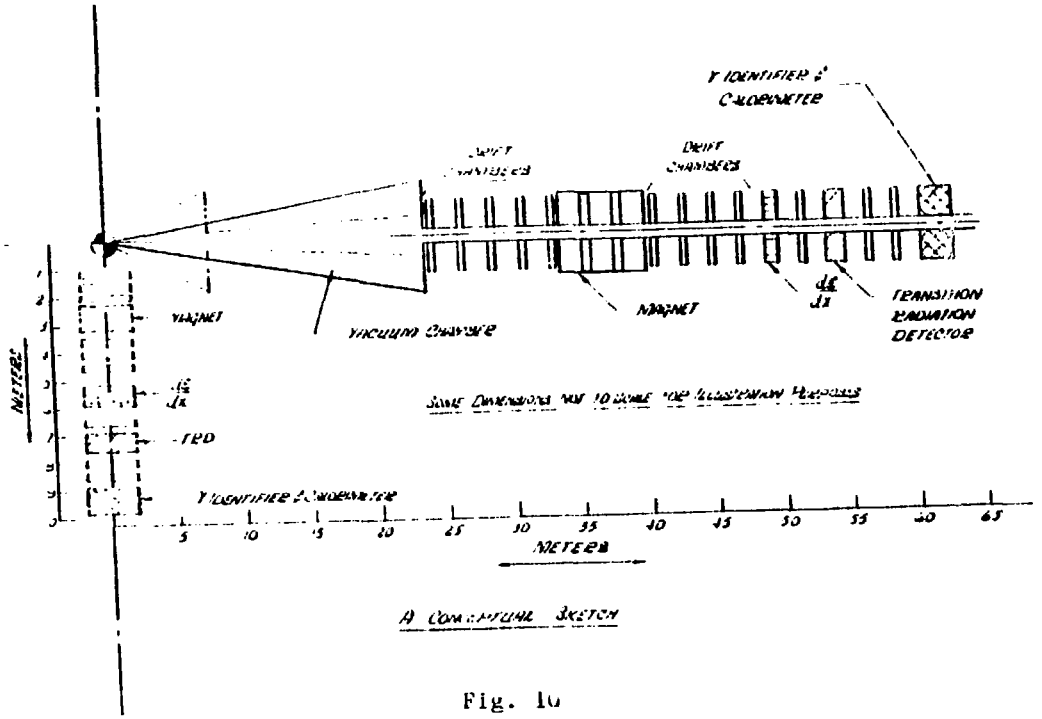
Y IDENTIFIER 2' CHLORINATED
DRIFT CHAMBERS
DRIFT CHAMBERS
MAGNET
MAGNET
VACUUM CHAMBER
TRANSITION RADIATION DETECTOR
METERS
FPD
Y IDENTIFIER 2 CHLORINATED
METERS
A CONCEPTUAL SKETCH

Fig. 10